Large Scale Domain Alignment of a Block Copolymer from Solution Using Electric Fields

Alexander Böker,[†,‡] Armin Knoll,[†] Hubert Elbs,[†] Volker Abetz,[‡] Axel H. E. Müller,[‡,§] and Georg Krausch*[,†,§]

Lehrstuhl für Physikalische Chemie II, Lehrstuhl für Makromolekulare Chemie II, and Bayreuther Zentrum für Kolloide und Grenzflächen, Universität Bayreuth, D-95440 Bayreuth, Germany

Received May 9, 2001

ABSTRACT: We have aligned the microdomains of a polystyrene-*b*-poly(2-hydroxyethyl methacrylate)-*b*-poly(methyl methacrylate) (PS-*b*-PHEMA-*b*-PMMA) triblock copolymer during preparation from solution by virtue of an external electric dc field (1.8 kV/mm). Bulk samples cast in the presence of an electric field exhibit lamellar microdomains highly oriented parallel to the electric field vector, as shown by small-angle X-ray scattering and transmission electron microscopy.

Introduction

The microphase separation of block copolymers has been studied extensively over the past two decades both experimentally and theoretically.[1,2] In the ordered state, these materials exhibit highly regular mesoscopic microdomain structures with characteristic length scales of the order of several tens of nanometers. Similar to polycrystalline materials, typically small grains of microdomains are formed, the size of which may be of the order of microns. As a consequence, although a single grain may have a highly anisotropic structure (e.g., in the case of cylindrical or lamellar structures), a bulk sample of a block copolymer typically exhibits isotropic materials properties. If macroscopic anisotropies are desirable, additional efforts have to be made to create macroscopic alignment of the microdomain structures. In the past, different techniques aiming toward macroscopic microdomain alignment have been devised. Most prominently, external mechanical fields have been successfully applied to orient block copolymer melts (e.g., large-amplitude oscillatory shear (LAOS)[3−5] or extrusion[6]) and block copolymer solutions (e.g., roll-casting[7]).

In addition to mechanical fields, the potential of electric fields for microdomain alignment has attracted increasing interest in the recent past as it may also be of considerable technical interest.[8] It has been shown that both lamellar and cylindrical microdomain structures in polystyrene-*b*-poly(methyl methacrylate) (PS-*b*-PMMA) melts could be oriented macroscopically by virtue of a dc electric field.[9−14] Because of the differences in the dielectric constants ($\Delta\epsilon$) of the blocks ($\epsilon_{PS} \approx 2.4$, $\epsilon_{PMMA} \approx 3.6$),[15] the microdomains tend to orient parallel to the electric field vector, thereby lowering the free energy of the system. The electric-field-induced driving force is proportional to $(\Delta\epsilon E)^2$.[10,14] Cylindrical microdomains can in principle be aligned along the field vector, resulting in a single monodomain (i.e., a block copolymer "single crystal"). In a lamellar microdomain structure, on the other hand, all lamellar orientations containing the electric field vector within the lamellar planes are energetically equivalent. Therefore, the electric field is expected to at best favor the subset of lamellar orientations with the lamellar normal pointing perpendicular to the field.

So far, most experiments using electric fields have been conducted in the melt. Because of the high melt viscosities, they are limited with respect to the molecular weight of the copolymers and the size of the macroscopic regions to be oriented ($M_w \approx 74\,000$ g/mol for thin films of thickness 1 μm;[16] $M_w \approx 37\,000$ g/mol for samples of thickness 2 mm[9,10]). In addition, temperatures close to the decomposition temperature and electric field strengths of up to 25 kV/mm are required to achieve high degrees of orientation. These limitations render the orientation of higher molecular weight copolymers or copolymers of more complex architectures (multiblock copolymers, star copolymers, etc.) rather difficult if not impossible, since their melt viscosities easily exceed the values faced in the investigations quoted above. Given the increasing interest in complex block copolymer structures, it is therefore desirable to explore alternative approaches, which circumvent the above limitations.

In the present contribution, we demonstrate the potential of an electric dc field for the microdomain alignment of a block copolymer *solution*.[17,18] The field is applied during solvent evaporation until final film formation and thereby leads to macroscopically oriented bulk specimens as well. The use of a solvent-based procedure extends the potential of electric fields for block copolymer alignment to a much larger class of block copolymers. As an example, we apply the approach to an ABC triblock copolymer, where macroscopic melt alignment in electric fields is expected to be hardly possible. We note that the aligning force of an electric field is significantly smaller for block copolymer solutions than for melts due to an effective reduction of the difference in the dielectric constants of the blocks $\Delta\epsilon$ by the solvent.

Experimental Section

A polystyrene-*b*-poly(2-hydroxyethyl methacrylate)-*b*-poly(methyl methacrylate) triblock copolymer was synthesized by

† Lehrstuhl für Physikalische Chemie II.
‡ Lehrstuhl für Makromolekulare Chemie II.
§ Bayreuther Zentrum für Kolloide und Grenzflächen.
* Corresponding author. E-mail: georg.krausch@uni-bayreuth.de.

10.1021/ma0108113 CCC: $22.00
Published on Web 01/18/2002

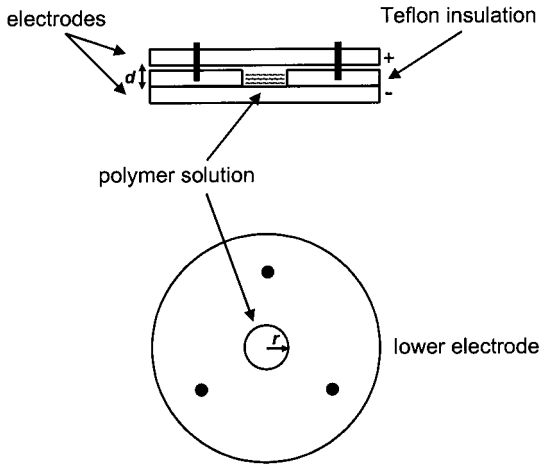

Figure 1. Capacitor setup used for sample preparation in the absence and in the presence of an electric field.

sequential living anionic polymerization as described in detail elsewhere.[19] The polymer used in this study consists of 47 wt % polystyrene, 43 wt % poly(methyl methacrylate) (PMMA), and 10 wt % poly(2-hydroxyethyl methacrylate) (PHEMA) with a total number-average molecular weight $M_n = 82\,000$ g/mol. GPC of the final block copolymer yields a polydispersity of $M_w/M_n = 1.04$.

Polymer Analysis. GPC measurements were performed using a set of 30 cm SDV-gel columns of 5 μm particle size having 10^5, 10^4, 10^3, and 10^2 Å pore size and dual detectors (RI and UV [$\lambda = 254$ nm]). The solvent was THF at room temperature with an elution rate of 1 mL/min. Narrowly distributed polystyrene samples were used as calibration standards.

^{1}H NMR spectra were acquired on a 250 MHz Bruker AC 250 instrument using $CDCl_3$ as solvent and tetramethylsilane (TMS) as internal standard. The molecular weights of the PHEMA and PMMA blocks were calculated using the block copolymer composition determined by NMR and the polystyrene molecular weight obtained from GPC.

Sample Preparation. The alignment experiments were performed in a cylindrical capacitor with aluminum electrodes ($r = 5$ mm, $d = 1.1$ mm; Figure 1) at room temperature. A dc voltage of 2 kV was applied resulting in an electric field strength of ~1.8 kV/mm. The voltage at the electrodes and the current were monitored during the course of the experiment, indicating only a small leakage current (0.01−0.02 mA) during the first few seconds after the field was applied. Between 0.2 and 1.1 mm thick films were obtained by slowly evaporating the solvent from 30 vol % solutions of the block copolymer in chloroform.

Small-Angle X-ray Scattering (SAXS). Cubic specimens of approximately 1 mm edge length were cut from the respective regions of interest of the as-cast film. SAXS measurements were performed using a Bruker-AXS Nanostar instrument with a sealed tube Cu K_α X-ray source ($\lambda = 1.5418$ Å) operated at 40 mA and 40 kV and a 2D Histar detector. The direction of the X-ray beam (approximate cross section: 100 μm/crossed Goebel mirrors) was perpendicular to the vector of the applied electric field. The scattering patterns were corrected for the beam stop and background prior to further evaluations.

To estimate the scattering contrast between PHEMA and PMMA, we calculate the electron density of both possible methacrylic phases taking into account the different densities of $\rho_{PHEMA} = 1.15$ g/cm^3 [15] and $\rho_{PMMA} = 1.19$ g/cm^3 [15] and the molecular weights of 130 and 100 g/mol, respectively. The calculations yield an electron density of 0.64 mol/cm^3 for PMMA and 0.62 mol/cm^3 for PHEMA. These values are similar and in both cases significantly higher than the 0.56 mol/cm^3 that we calculate for the polystyrene phase. Therefore, we may conclude that there is no significant scattering contrast between the methacrylic phases compared to polystyrene.

Scanning Electron Microscopy (SEM). SEM was performed using a LEO 1530 Gemini instrument equipped with a field emission cathode with a lateral resolution of approximately 2 nm. The acceleration voltage was 5 kV. The sample was prepared by freeze fracture. Prior to the measurements it was sputtered with gold.

Transmission Electron Microscopy (TEM). Thin sections were cut from the as-cast films parallel to the electric field vector (far from any surface) using a Reichert-Jung Ultracut E microtome equipped with a diamond knife. To enhance the electron density contrast between polystyrene and the methacrylic blocks, the sections were exposed to RuO_4 vapor for 45 min, which leads to a preferential staining of the polystyrene block.[20] Bright field TEM was performed using a Zeiss electron microscope (CEM 902) operated at 80 kV in the bright field mode.

Calculation of Order Parameters. As will become clear from the experimental observations described below, domain alignment is induced by two competing external fields of different symmetry, i.e., the interfacial field between polymer solution and electrode surface and the electric field, respectively. To quantify the alignment, we calculate the order parameter P_2 by integrating the scattering intensity from $\varphi = 0°$ to 360°:

$$P_2 = \frac{3\langle\cos^2\varphi\rangle - 1}{2}$$

with

$$\langle\cos^2\varphi\rangle = \frac{\int_0^{2\pi} d\varphi\, (I_q(\varphi)\cos^2(\varphi)\,|\sin(\varphi)|)}{\int_0^{2\pi} d\varphi\, (I_q(\varphi)|\sin(\varphi)|)}$$

Depending on the position of the maxima of the scattering intensity, the calculation yields two different ranges of the order parameter. For lamellar alignment parallel to the electrodes (maximum at $\varphi = 0°$), P_2 ranges from 0 to 1 with $P_2 = 1$ corresponding to perfect lamellar alignment where all lamellar normals are oriented perpendicular to the surfaces, i.e., electrodes. For alignment of the lamellae along the field direction (maximum at $\varphi = 90°$), P_2 ranges from 0 to −0.5 with $P_2 = -0.5$ corresponding to the case where all lamellae are aligned parallel to the field, however, with the lamella normals being isotropically oriented in the plane of the electrodes. Depending on the type of alignment, the maximum values describing perfect alignment are 1 and −0.5.

Results

Films Cast at Zero Electric Field. To exclude any effect of solvent evaporation on the alignment process, films were cast in the setup shown in Figure 1, however in the absence of an external electric field. We observe a highly anisotropic SAXS pattern as shown in Figure 2A. The azimuthal angular dependence (φ) of the scattering intensity (Figure 2B) reveals a preferential alignment of the lamellae parallel to the electrodes. We attribute this finding to a strong affinity of the solution/electrode interface to one of the blocks, which leads to preferential orientation of the lamellae parallel to the electrodes during solvent evaporation. This phenomenon has already been observed by Annighöfer and Gronski for controlled solvent casting of lamellar polystyrene-*b*-polyisoprene diblock copolymers.[21]

For the data presented in Figure 2 we calculate the order parameter of $P_2 = 0.43$. The lamellar spacing $d_{SAXS} = 45 \pm 2$ nm calculated from the first-order reflection in Figure 2C at $q^* = 0.14$ nm^{-1} ($d_{SAXS} = 2\pi/q^*$) fits well to the value $d_{TEM} = 40 \pm 2$ nm obtained from the TEM pictures (Figure 3A). Furthermore, Figure 3A shows a well-ordered lamellar microdomain

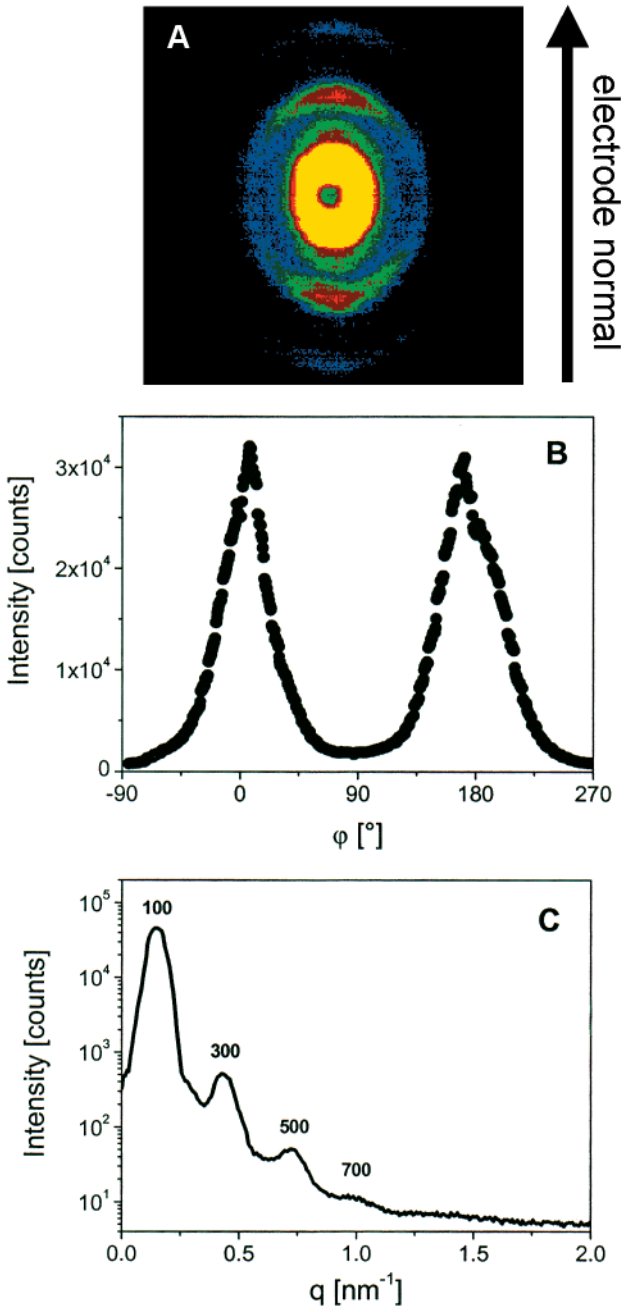

Figure 2. (A) 2D-SAXS pattern of a film cast under zero-field conditions. The lamellae are aligned parallel to the boundary surfaces (electrodes). (B) Azimuthal intensity distribution at $q^* = 0.14$ nm^{-1} (corresponding to first-order reflection). (C) Azimuthally integrated intensity as a function of scattering vector q.

alignment parallel to the electrode surfaces, thereby corroborating the SAXS results.

Films Cast in the Presence of an Electric Field. Film formation under the influence of an external electric field results in significant thickness undulations, which eventually lead to the formation of columnlike protrusions that connect both electrodes. Recently, Schäffer et al. showed that electric fields can induce instabilities in a liquid polymer film leading to the formation of polymer columns quite similar to the ones observed here.[22,23] Aside from the columns, we find areas with film thicknesses ranging between 0.2 and 0.7 mm. All these parts show a significant alignment of the lamellae parallel to the electric field. The most

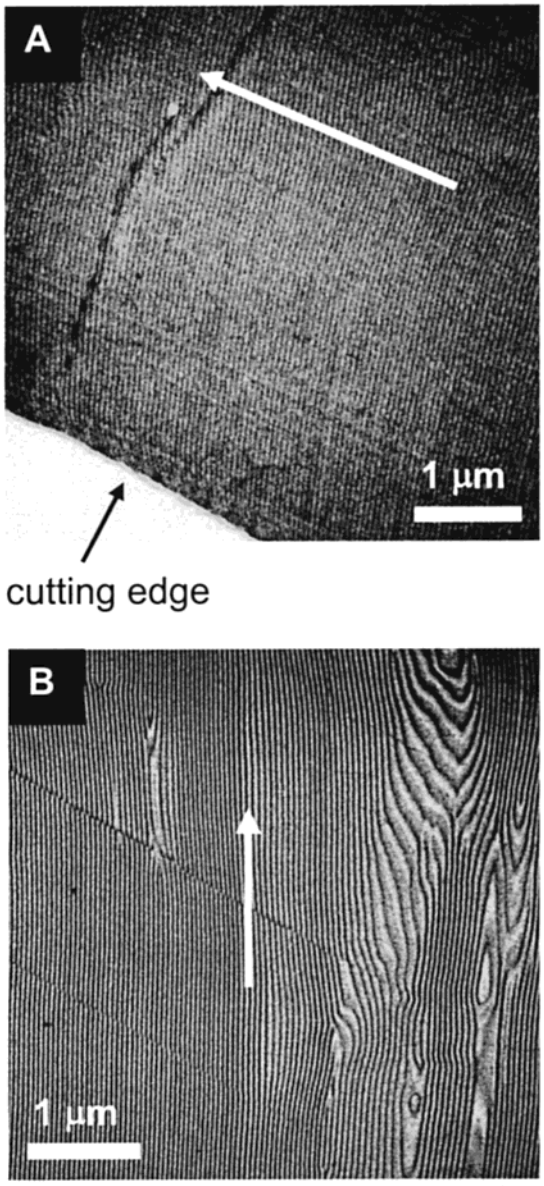

Figure 3. TEM pictures of zero-field and alignment experiment: (A) zero field (the arrow indicates the direction perpendicular to the electrodes); (B) $E = 1.8$ kV/mm (the arrow indicates the direction of the electric field vector). The image was taken from one of the columns bridging between the electrodes.

pronounced anisotropy, however, is found in the columnar protrusions on which we will focus in the present study. Figure 4 shows a cross-sectional SEM image of a typical column. The curvature of the boundaries is induced by the wetting of the electrode surfaces during evolution of the protrusion.

A representative SAXS pattern taken within one of the columns is shown in Figure 5A. It reveals an anisotropic azimuthal angular dependence of the scattering intensities (Figure 5B) shifted by 90° compared to the zero-field experiment. The Bragg reflections are identical to the ones observed in the zero-field experiment. The order parameter P_2 yields -0.4. Thus, these results clearly indicate a predominant alignment of the lamellae parallel to the electric field vector. A representative TEM picture is shown in Figure 3B. There are regions of very uniform lamellae aligned parallel to the electric field vector throughout the whole picture.

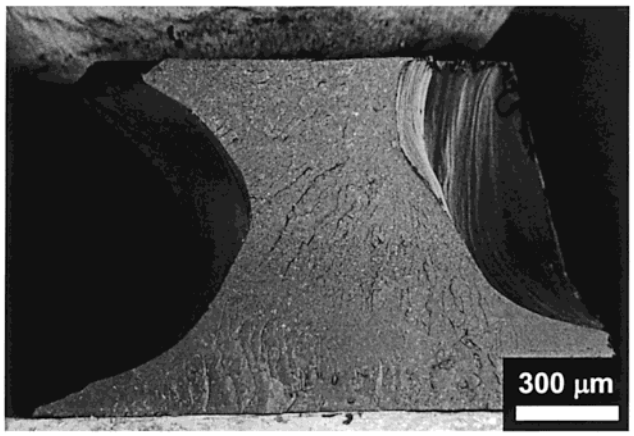

Figure 4. Cross-sectional SEM image of a protrusion formed during exposure to a dc electric field (1.8 kV/mm).

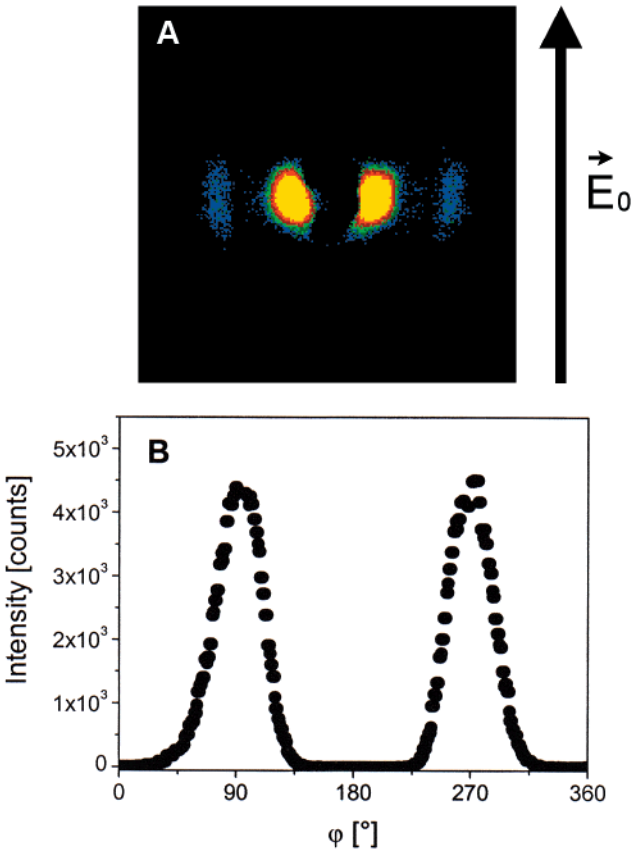

Figure 5. (A) 2D-SAXS pattern of a film cast in the presence of a dc electric field (1.8 kV/mm). The experiment has been performed within one of the columns bridging between the electrodes. The lamellae are oriented preferentially along the field direction. (B) Azimuthal intensity distribution at first-order reflection.

Interestingly, the orientation of these lamellae is not disturbed by the defect structures (e.g., disclinations). Furthermore, it appears that the trajectories of the disclination lines and other defects (coarse patterns similar to wood grain patterns) are aligned predominantly in the direction of the electric field as well. Especially the latter defects have been reported earlier for PS-*b*-PMMA block copolymers oriented in an electric field from the melt. These structures may arise from disclination lines cut shallowly parallel to their trajectories.[24] Investigations of the lamellar alignment at the film boundaries reveal the large influence of the electrode surface on the microdomain alignment as has already been observed for the zero-field experiment. Even with an applied electric field, we find orientation of the lamellae parallel to the electrode surface for the first 10−40 lamellar layers as shown in Figure 6.

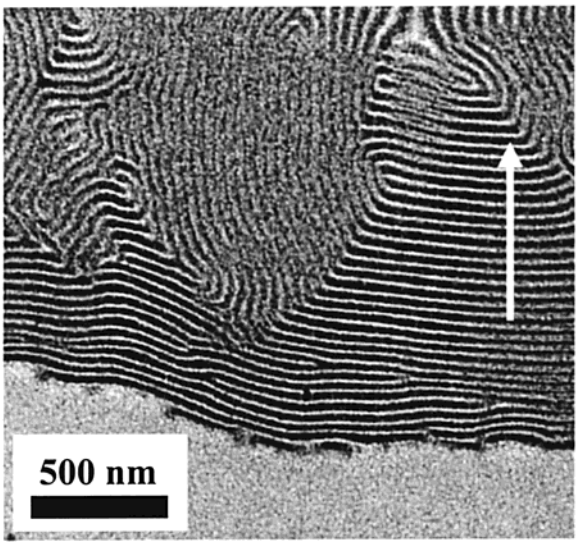

Figure 6. TEM picture of interfacial region between electric field aligned polymer film and electrode surface (film embedded in epoxy resin; the arrow indicates the direction of the electric field vector).

Discussion

We start our discussion with a quantitative estimate of the energies involved in the process of domain ordering in our experiments. For this end we note that we have evidence that the PHEMA block is actually miscible with the PMMA block. This is indicated by differential scanning calorimetry (DSC) and rheological and TEM experiments, where only a single methacrylic phase could be identified. TEM experiments involved the staining with phosphotungstic acid and long time exposure to ruthenium tetroxide vapor which is well-known to lead not only to staining of the PS block but also should react with hydroxyl groups.[20] As both methods did not lead to definite results and DSC and rheological measurements only revealed two glass transition temperatures at 110 and 137 °C which are attributed to the PS and a methacrylic phase, respectively, we anticipate that PHEMA and PMMA may form a mixed phase.

This assumption leads us to treat the triblock copolymer as an AB diblock copolymer with the following composition: (A) 47 wt % PS ($\epsilon_A = 2.4$) and (B) 53 wt % methacrylic blocks ($\epsilon_B = 0.81\epsilon_{PMMA} + 0.19\epsilon_{PHEMA} = 4.6$; with $\epsilon_{PMMA} = 3.6$ and $\epsilon_{PHEMA} = 8.9$[25]). As chloroform ($\epsilon_{CHCl_3} \approx 4.8$) is a fairly nonselective solvent for the two main components, PS and PMMA, we expect a similar swelling behavior leading merely to a dilution effect with respect to the dielectric constants of each block. Therefore, with increasing solvent content in the films, the difference of the dielectric constants is reduced, and the thermodynamic driving force for an alignment of the lamellae parallel to the field is expected to decrease.[14] As has been pointed out by Amundson et al.[10] with respect to melts of PS-*b*-PMMA block copolymers, this force is already small, so that it is remarkable that its decrease still leaves a sufficient driving force to allow for preferential alignment of the microdomains.

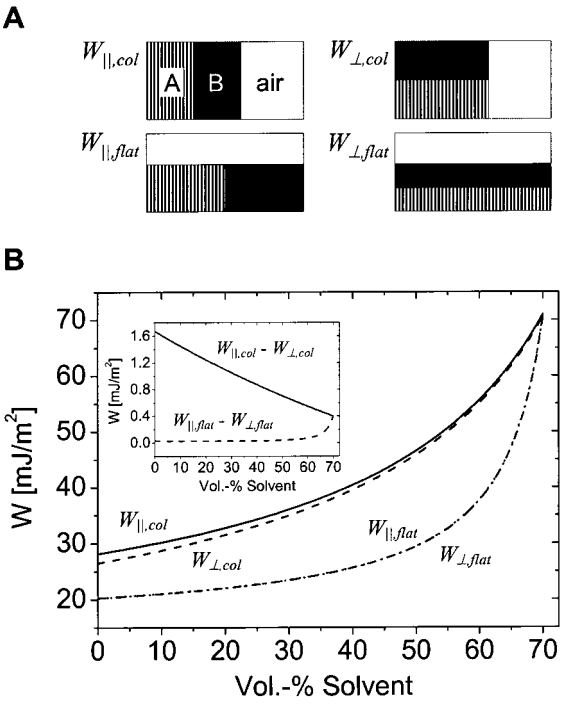

Figure 7. (A) Different geometries used for the calculation of the electric energy W stored in a capacitor partially filled with polymers A and B. (B) Energy per area stored in the capacitor for the four geometries as a function of solvent concentration. The inset shows the energy difference between the two orientations for columns ($W_{||,col} - W_{\perp,col}$) and for a flat film ($W_{||,flat} - W_{\perp,flat}$).

To estimate the driving forces for domain alignment as a function of solvent concentration ϕ, we calculate the electric energy per unit area W, which is stored in the capacitor for the different situations sketched in Figure 7A. The model relies on two major assumptions: The dielectric constant of a mixture ϵ_{mix} of polymer ϵ_{pol} and solvent ϵ_{sol} is assumed to depend linearly on the solvent concentration ϕ:

$$\epsilon_{mix} = \phi\epsilon_{sol} + (1 - \phi)\epsilon_{pol}$$

We further disregard any influence of the solvent on the partial molar volume of the polymer, i.e., the volumes of polymer V_{pol} and solvent V_{sol} simply add:

$$V_{mix} = V_{pol} + V_{sol}$$

Four basic geometries have been identified to describe the system, corresponding to a perpendicular ($W_{\perp,col}$, $W_{\perp,flat}$) and parallel ($W_{||,col}$, $W_{||,flat}$) alignment of the microdomains with respect to the electric field and to a formation of columns ($W_{\perp,col}$, $W_{||,col}$) and a flat film ($W_{\perp,flat}$, $W_{||,flat}$), respectively.

We calculate the energy W stored within the electric field of the capacitor according to

$$W = {}^1/_2\int \vec{E}\cdot\vec{D}\, dV$$

with $\vec{E}$ being the electric field and $\vec{D}$ the displacement field.

In contrast to the dielectric displacement $\vec{D}$, the electric field $\vec{E}$ along the z-direction of the capacitor is not uniform for the models, which incorporate a layered structure ($W_{\perp,flat}$ and $W_{\perp,col}$). This is due to the fact that the component of the electric field perpendicular to the interface between two materials is not continuous, but the one of the displacement field is ($\vec{D}_{\perp 1} = \vec{D}_{\perp 2}$ but $\vec{E}_{\perp 1} \neq \vec{E}_{\perp 2}$). Additionally, $\vec{E}_i = \vec{D}_i/\epsilon_i$ and the applied voltage $V = \int E\, dz$, which means that as soon as air is present as a layer in the capacitor with the applied voltage V, the electric field in both polymer layers is reduced. This leads effectively to a reduced energy stored inside the capacitor and to a reduced alignment of the block copolymer in the thinner parts of the sample. We are well aware of the fact that our calculations neglect the existence of interfacial boundary regions in concentrated polymer solutions. Therefore, the results may represent an approximation to the upper limit of the real energetic situation.

Figure 7B shows the energy per unit area stored inside a capacitor filled with 15 vol % polymer A ($\epsilon_A = 2.4$) and 15 vol % polymer B ($\epsilon_B = 4.6$) as a function of solvent volume fraction ($\epsilon_{sol} = 4.8$), corresponding to the four basic geometries, with a gap width of 1.1 mm and an applied voltage of 2 kV.

Curves $W_{\perp,col}$ and $W_{\perp,flat}$ as well as curves $W_{||,col}$ and $W_{||,flat}$ converge at a solvent concentration of 70 vol % (which is the starting concentration of our experiment), because at this point the capacitor is completely filled and the respective geometries are equivalent. For the major part of the plot, columns ($W_{\perp,col}$, $W_{||,col}$) store more energy than flat films ($W_{\perp,flat}$, $W_{||,flat}$) because the polymer/solvent mixture exhibits a higher dielectric constant as compared to that of air. Therefore, column formation should be favored in agreement with the experimental finding. It has to be kept in mind though that column formation requires the formation of additional surfaces, which leads to an energy penalty. Obviously, according to our results, the gain in energy during alignment of the lamellae parallel to the electric field vector is large enough to compensate for an additional surface energy cost. An approximation taking into account the dimensions of the observed protrusions, a mean surface energy of ~30 mJ/m^2 ($\gamma_{PS} = 40.7$ mJ/m^2, $\gamma_{PMMA} = 41.1$ mJ/m^2, $\gamma_{CHCl_3} = 26.7$ mJ/m^2),[15] and the gain in electric energy per unit area in the capacitor (~20 mJ/m^2 at 50−60 vol % solvent) leads to the following result: At a certain ratio of the radius R of a column to its height H ($R/H \sim 0.8$), the surface and electric energy contributions are equal. Given the fact that the columns observed in our experiment start to evolve at relatively high solvent concentrations, we have to consider a significant shrinkage in the lateral dimensions during film formation. However, the gain in electric energy for the aligned system is of the same order of magnitude as the surface energy cost. The observation that we still find material in between the protrusions can be explained by the fact that the overall process of film formation, i.e., drying of the polymer solution, occurs at a faster rate than the formation of the columns.

The electric energies for structures aligned parallel to the electric field are always larger than the ones for structures oriented perpendicular to the field, explaining the preferential alignment observed in the experiment. It is interesting to look at the energy difference between the microdomain orientations in the columns ($W_{\perp,col}$, $W_{||,col}$) and the one in the flat film ($W_{\perp,flat}$, $W_{||,flat}$), which is shown in the inset in Figure 7B. With decreasing solvent concentration this value is much higher for the columns. Therefore, the microdomain ordering inside the columns is expected to be better than inside

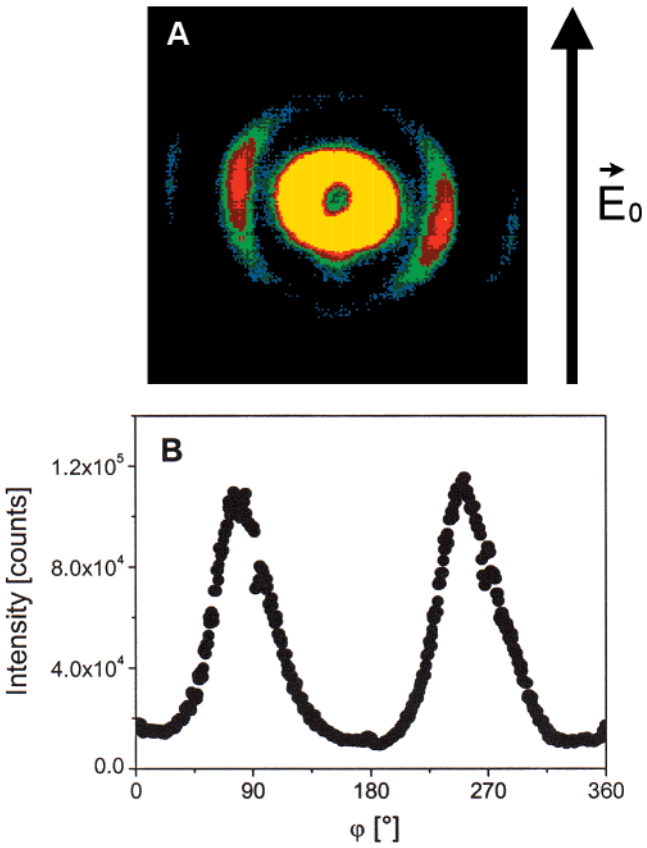

Figure 8. (A) SAXS pattern of a sample taken from the flat areas in between the columns. The lamellae are oriented along the field direction (1.8 kV/mm); however, the degree of order as calculated by the azimuthal angular dependence of the scattering intensity (B) is smaller than within the columns ($P_2 = -0.25$ compared to -0.4).

the flat film regions in between the columns. In addition, for the case of the thinner films in between the columns we expect a larger influence of the electrode/polymer and the polymer/air interfaces, which would favor lamellar alignment parallel to the electrodes. These two effects are in competition, and only if the electric field is large enough the microdomains will align parallel to the field.[14] Indeed, SAXS experiments performed in the flat areas in between the columns (Figure 8) show a lamellar alignment along the field direction, however, with a significantly smaller degree of order ($P_2 = -0.25$).

There have been various assumptions concerning the mechanism of microdomain alignment, which are mostly based on defect movement, resulting in either mutual annihilation of equivalent defects (which are traverse to the electric field) or pinning of defect structures.[10,24] This would lead to clustering of defects and orientation along the electric field direction, which is consistent with our results as it explains why we do not reach "perfect" alignment of the lamellar microdomains. Nevertheless, the application of an external electric field to a block copolymer solution is capable of switching the in-plane alignment of the lamellae induced by the boundary surfaces to a significant orientation along the electric field direction. Investigations on the kinetics of this process are presently under way and will be presented in a separate publication.[26]

As the alignment of the microstructure takes place during solvent evaporation and along with a change of the macroscopic shape of the specimen (protrusions), we have to consider the potential effect of shear forces. Therefore, the following control experiment was performed: The distance between the electrodes was doubled, and the same voltage as before was applied to the system (which results in half the electric field strength as before). While protrusions were formed as described above, no alignment of the microdomains along the electric field was found under these conditions. We therefore exclude shear as the dominant driving force for domain alignment in our experiments.

Finally, we note that although we can model our system as a diblock copolymer in our calculations, the incorporation of the PHEMA middle block seems to be essential for the ordering process to function. Similar experiments on PS-*b*-PMMA diblock copolymer solutions (not shown here) did *not* exhibit field-induced domain alignment. Two reasons may be responsible for this observation: At first, the high dielectric constant of PHEMA ($\epsilon_{PMMA} = 8.9$) significantly increases the driving force for ordering even at the rather small volume fraction realized in the present experiments. Moreover, microphase separation in PS-*b*-PMMA diblock copolymer solutions occurs only at polymer concentrations above 60 wt %, while the PHEMA containing triblock copolymers already microphase separate at polymer concentrations around 40 wt %. In the latter case, the viscosity of the phase separated solution is considerably smaller which helps the ordering process induced by the small electric force. Recent kinectic experiments indicate that there is a rather small concentration window in which microdomain ordering by electric fields can effectively be realized. This issue will be subject of a forthcoming publication.[26] The use of a PS-*b*-PHEMA diblock copolymer as a model system, however, is not suitable, as PHEMA exhibits a very strong surface interaction with the electrode material, and its amphiphilic character leads to a selective solubility in all low dielectric constant solvents, which would further complicate the situation.

Conclusions

We have shown that block copolymer solutions can be aligned in dc electric fields during solvent evaporation, leading to highly anisotropic microdomain structures in the resulting films. In comparison to melt alignment, the method presented here is applicable to polymers with higher melt viscosities such as high molecular weight copolymers and copolymers of more complex architecture, which cannot be aligned in the melt by virtue of electric fields.

Furthermore, we were able to describe the observed behavior by a quantitative estimate of the electric energies involved in the alignment process. Our calculations predict the formation of columnlike protrusions during solvent evaporation and explain the higher degree of orientation found in the columns as compared to the thinner parts of the films.

Future work will have to concentrate on a quantitative control of the solvent vapor pressure during orientation of the domains. There should exist an optimum degree of swelling around the order−disorder concentration, which combines a maximum chain mobility with a significant energetic difference between the different microdomain orientations. Keeping the system at the respective vapor pressure (i.e., concentration of the polymer solution) for a sufficient time should result in a significant improvement of the long-range order of the microdomains.

Acknowledgment. The authors thank C. Drummer, A. Göpfert, and S. Stangler for their skillful help with the SEM, TEM, and SAXS measurements, respectively. We thank M. Hund for his assistance devising the capacitor setup. A.B. acknowledges helpful discussions with H. Schmalz and a Kekulé fellowship by the Stiftung Stipendien-Fonds des Verbandes der Chemischen Industrie and the German Bundesministerium für Bildung und Forschung (BMBF). This work was carried out in the framework of the Sonderforschungsbereich 481 funded by the German Science Foundation (DFG).

References and Notes

(1) Bates, F. S.; Fredrickson, G. H. *Annu. Rev. Phys. Chem.* **1990**, *41*, 525.
(2) Bates, F. S.; Frederickson, G. H. *Phys. Today* **1999**, *52*, 32.
(3) Wiesner, U. *Macromol. Chem. Phys.* **1997**, *198*, 3319.
(4) Chen, Z.-R.; Kornfield, J. A.; Smith, S. D.; Grothaus, J. T.; Satkowski, M. M.; *Science* **1997**, *277*, 1248.
(5) Chen, Z.-R.; Kornfield, J. A. *Polymer* **1998**, *39*, 4679.
(6) Keller, A.; Pedemonte, E.; Willmouth, F. M. *Nature* **1970**, *225*, 538.
(7) Albalak, R. J.; Thomas, E. L. *J. Polym. Sci., Polym. Phys. Ed.* **1993**, *31*, 37.
(8) Thurn-Albrecht, T.; Schotter, J.; Kastle, G. A.; Emley, N.; Shibauchi, T.; Krusin-Elbaum, L.; Guarini, K.; Black, C. T.; Tuominen, M. T.; Russell, T. P. *Science* **2000**, *290*, 2126.
(9) Amundson, K.; Helfand, E.; Davis, D. D.; Quan, X.; Patel, S. S.; Smith, S. D. *Macromolecules* **1991**, *24*, 6546.
(10) Amundson, K.; Helfand, E.; Quan, X.; Smith, S. D. *Macromolecules*, **1993**, *26*, 2698.
(11) Morkved, T. L.; Lu, M.; Urbas, A. M.; Ehrichs, E. E.; Jaeger, H. M.; Mansky, P.; Russell, T. P. *Science*, **1996**, *273*, 931.
(12) Morkved, T. L.; Lopez, V. A.; Hahm, J.; Sibener, S. J.; Jaeger, H. M. *Polymer* **1998**, *39*, 3871.
(13) Mansky, P.; DeRouchey, J.; Russell, T. P.; Mays, J.; Pitsikalis, M.; Morkved, T. L.; Jaeger, H. M. *Macromolecules*, **1998**, *31*, 4399.
(14) Thurn-Albrecht, T.; DeRouchey, J.; Russell, T. P.; Jaeger, H. M. *Macromolecules* **2000**, *33*, 3250.
(15) Brandrup, J.; Immergut, E. H. *Polymer Handbook*, 3rd ed.; Wiley: New York, 1991.
(16) Thurn-Albrecht, T.; Steiner, R.; DeRouchey, J.; Stafford, C. M.; Huang, E.; Bal, M.; Tuominen, M.; Hawker, C. J.; Russell, T. P. *Adv. Mater.* **2000**, *12*, 787.
(17) Le Meur, J.; Terrisse, J.; Schwab, C.; Goldzene, P. *J. Phys., Colloq.* **1971**, *32*, C5a-301.
(18) Serpico, J. M.; Wnek, G. E.; Krause, S.; Smith, T. W.; Luca, D. J.; van Laeken, A. *Macromolecules* **1992**, *25*, 6373.
(19) Böker, A.; Müller, A. H. E.; Krausch, G. *Macromolecules* **2001**, *34*, 7477.
(20) Sawyer, C. C.; Grubb, D. T. *Polymer Microscopy*, 2nd ed.; Chapman & Hall: London, 1996.
(21) Annighöfer, F.; Gronski, W. *Makromol. Chem., Rapid Commun.* **1983**, *4*, 123.
(22) Schäffer, E.; Thurn-Albrecht, T.; Russell, T. P.; Steiner, U. *Nature* **2000**, *403*, 874.
(23) Lin, Z.; Kerle, T.; Baker, S. M.; Hoagland, D. A.; Schäffer, E.; Steiner, U.; Russell, T. P. *J. Chem. Phys.* **2001**, *14*, 2377.
(24) Amundson, K.; Helfand, E.; Quan, X.; Hudson, S. D.; Smith, S. D. *Macromolecules* **1994**, *27*, 6559.
(25) Yamaguchi, R.; Sato, S. *Jpn. J. Appl. Phys.* **1994**, *33*, 4007.
(26) Böker, A.; Elbs, H.; Hänsel, H.; Knoll, A.; Zettl, H.; Urban, V.; Abetz, V.; Müller, A. H. E.; Krausch, G. Manuscript in preparation.

MA0108113